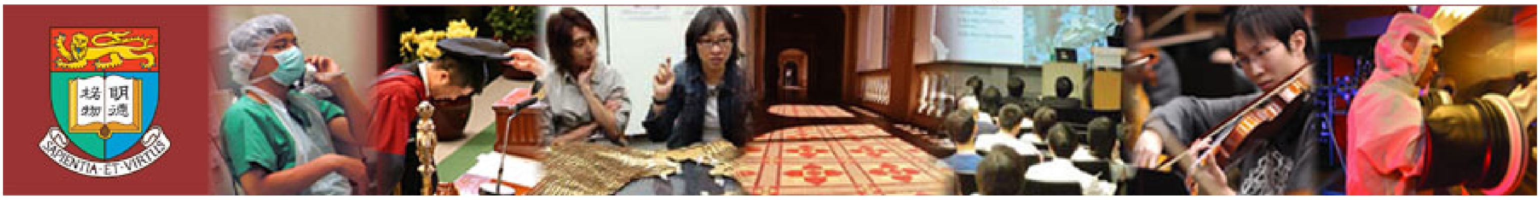

Title	**Dosimetric evaluation of the interplay between LINAC movement and tumor motion in respiratory gated VMAT of lung cancer**
Author(s)	**Ng, CY; Lee, VHF; Leung, TW**
Citation	**The 54th Annual Meeting of the American Society for Radiation Oncology, Boston, MA., 28 October-1 November 2012. In Radiation Oncology, 2012, v. 84 n. 3 suppl., p. S766-S767, abstract no. 3458**
Issued Date	**2012**
URL	**http://hdl.handle.net/10722/165596**
Rights	**Radiation Oncology. Copyright © BioMed Central Ltd.**

to reveal the event and error frequency. Additionally, the possible causes of the errors and possible effective countermeasures were considered.

Materials/Methods: In our hospital, the treatment plans made mostly by radiation oncologists are checked by two medical physicists using a chart check implemented in an electronic health record system. If the physicist detects the errors in TPS-stage, the detector completes the near-incident and incident report, and these reports are submitted to monthly radiation safety conference. All of the staffs involved in radiation therapy attend the conference and information of the new errors and the possible countermeasures will be informed to all the staffs. The 5513 treatment plans between May 2007 and December 2011 were checked before the treatments.

Results: Of the 5513 treatment plans, all of the 376 errors were detected before the actual delivery of irradiation. Average error probability of 7% was obtained. That means that, approximately 7 out of 100 treatment plans have something wrong in the TPS-stage: Table shows the errors with a higher probability. "MLC/Jaw" is one relating to mis-setting the field size with the collimator jaws and multi-leaf collimators (MLC). "Dose/fraction" is one relating to mis-setting dose and fraction, e.g., prescribed dose is not equal to the sum of dose of each field. "Isocenter/Reference point" is one relating to mis-locations of isocenter and reference point (not ICRU prescription, etc). Some examples of countermeasures are the feedback of these results to the planner to prevent the errors, the training for the staffs, and the utilizing manual describing the pit-falls in the operation of the TPS.

Poster Viewing Abstract 3456; Table Classification of the 372 errors in 5513 treatment plans

Error	Probability	Number of events
Jaw/MLC	1.5%	83
Machine ID	1.2%	65
Dose/fraction	0.9%	49
Isocenter/Reference point	0.8%	42
Bolus	0.2%	12
Algorithm	0.2%	11
Heterogeneity correction	0.2%	10
Others	1.8%	100
Total	6.7%	372

Conclusion: It is more important to establish the system of completely detecting the unexpected errors by "Robust QA program". The errors in the TPS-stage should be shared with not only the radiation oncologists as planners, but also with medical physicists and radiation technologists, and the other staffs involved in radiation therapy, which lead to create "safety culture" in the department.

Author Disclosure: H. Okamoto: None. A. Wakita: None. M. Kawashima: None. Y. Saitoh: None. A. Aikawa: None. M. Fuse: None. Y. Abe: None. Y. Itou: None. M. Sumi: None. J. Itami: None.

3457

The Application of Metal Artifact Reduction Algorithm in CT Spectral Imaging on Radiation Therapy Dose Calculation

H. Geng, S. Yu, K. Cheung, W. Lam, and S.G. Lo; *Hong Kong Sanatorium & Hospital, Hong Kong, Hong Kong*

Purpose/Objective(s): To evaluated the effect of applying metal artifact reduction technique using CT spectral imaging on radiation therapy dose calculation.

Materials/Methods: A cylindrical phantom (20cm long with 15cm diameter) implanted with four stainless steel inserts (4.5cm long with 0.4cm diameter) was used in this study. The inserts were positioned symmetrically 1.5cm from the central axis of the phantom. The phantom with metallic inserts was scanned on a dual-energy CT scanner using both conventional 120kVp technique and spectral imaging technique. 140keV monochromatic images applied with metal artifact reduction algorithm were also reconstructed. The variation of CT number in central region of the phantom surrounded by the metallic inserts was assessed for both image sets. As standard for comparison, an artifact-free image set was created by scanning the phantom without metallic inserts using 120kVp technique and assigning the density of stainless steel to the inserts' locations on the phantom images. A cylindrical target volume (3cm long with 2cm diameter) was defined in the center of the phantom. A volumetric modulated arc therapy plan was generated on the artifact-free images. The same plan was copied and applied to both 120kVp images and 140keV monochromatic images. Dose differences calculated from different images were evaluated and compared with the actual dose measurements using an ionization chamber and radiochromic film.

Results: Serious metallic artifacts were observed in the 120kVp images, with CT numbers in the central region of the phantom varied from -1000HU to 766HU (mean = 14.6HU, SD = 459.6). The metallic artifacts were significantly reduced in the 140keV images, with CT numbers varied from 126HU to 171HU (mean = 152.4HU, SD = 8.9). These variations in CT number contributed to the variation in relative electron density from 0 to 1.44 and from 1.12 to 1.16, respectively, whereas the expected electron density was 1.11 as measured in the standard artifact-free images. Comparing to radiochromic film measurement, the dose distributions calculated using these three image sets were all within 3%/3mm tolerance in gamma analysis. The deviations between measured and calculated dose using three image sets were all less than ±1%.

Conclusions: The metal artifact reduction algorithm in CT spectral imaging technique can significantly reduce the metallic artifacts, which may help to improve the accuracy in dose calculation and delineation of tumors and critical structures. But for small objects, the improvement in dosimetric accuracy was not significant.

Author Disclosure: H. Geng: None. S. Yu: None. K. Cheung: None. W. Lam: None. S.G. Lo: None.

3458

Dosimetric Evaluation of the Interplay Between LINAC Movement and Tumor Motion in Respiratory Gated VMAT of Lung Cancer

C. Ng, V.H. Lee, and T. Leung; *Queen Mary Hospital, Hong Kong, Hong Kong*

Purpose/Objective(s): Respiratory gated radiation therapy of lung cancer helps to minimize the treated volume and hence treatment side effects. VMAT can reduce the treatment time while producing a highly conformed dose distribution. However, in gated VMAT delivery, the interplay effect between the LINAC movement (MLC and gantry) and tumor motion may result in undesirable hot and cold spots jeopardizing tumor coverage. In this study we investigated the possible dosimetric errors caused by the interplay between the tumor motion and the LINAC movement for gated VMAT lung cancer treatment.

Materials/Methods: We studied 2 lung cancer cases prescribed to 60 Gy given in 30 fractions. GTVs were contoured on each of the 10 phases of 4DCT. The end-expiration phase and 3 neighboring phases were chosen for gating (40%-70%). The GTV_{gating} consisted of the volume encompassing GTVs of the 4 phases. 5 mm margin was added to the GTV_{gating} to create the CTV_{gating} and 8 mm margin was added to generate the PTV_{gating}. A highly modulated single arc VMAT plan was derived for each case based on the 50% phase image. The plans aimed to minimize dose to the spinal cord while maintaining PTV coverage. A program was written to segment the arc in the original plan with 177 control points into 88 mini arcs with 3 control points each. Each mini arc spanned about 0.67 second and was assumed to irradiate 1 phase of the gating window during which there should be relatively little movement of the anatomy. Every one in four arcs was then inserted into a VMAT plan irradiating each of the 4 phases, thus generating 4 plans each having 22 mini arcs. Dose calculation was done for each plan on the CT image for the particular phase. The resulting dose from each plan was then mapped to the base phase image (50%) and finally summed with a deformable dose accumulation software. The resulting dose was compared to the original dose distribution.

Results: See Table.

Conclusion: The dosimetric effect of the interplay between tumor motion and LINAC movement was studied for 2 lung cancer cases. It was found that there was no significant difference in tumor coverage when the original plan was done assuming a static target. The dose to critical structures also remained very close to the original plan. It can be concluded that

Poster Viewing Abstract 3458; Table Summary of dosimetric results

	Plan	PTV vol (cc)	PTV D95% (Gy)	PTV D1% (Gy)	Mean lung dose (Gy)	Spinal cord D1% (Gy)
Case 1	VMAT	254.8	60.0	65.7	19.2	41.6
	Sum 4 Phase Plan	254.8	59.7	66.0	19.3	41.0
Case 2	VMAT	22.7	60.6	63.9	7.0	7.0
	Sum 4 Phase Plan	22.7	60.1	63.9	7.0	7.3

interplay between LINAC movement and tumor motion will not affect the dosimetric quality of gated VMAT plans for lung cancer.

Author Disclosure: C. Ng: None. V.H. Lee: None. T. Leung: None.

3459

MVCT-Detector-based Dose Reconstruction Makes Phantom QA Measurements for Tomotherapy Prostate Treatments Redundant

T. Nuver, D. Kramer, V. Althof, R. Westendorp, and A. Minken; *RISO, Deventer, Netherlands*

Purpose/Objective(s): (1) To reconstruct delivered dose for prostate patients treated on a tomotherapy unit based on measurements with the integrated MVCT-detector array. (2) To report the first clinical experiences using first fraction dose reconstruction instead of pre-treatment phantom measurements.

Materials/Methods: Dose verification software tools were used to compare reconstructed delivered dose with planned dose. Fractionation schedules varied from 2.3 to 2.9 Gy, depending on tumor stage. Treatment plans were generated on two versions of tomotherapy TPS (69 patients [version 1] and13 patients [version 2], respectively). All patients were positioned based on daily, on-line MVCT scans using implanted gold markers. The detector signals were attenuation corrected based on the planning kVCT scan to reconstruct the incoming fluence. This fluence was then re-projected on the kVCT scan to calculate delivered dose. The planned dose distribution was subtracted from the reconstructed distribution. Histograms were constructed from the local dose differences. Only voxels with a planned dose larger than 80% of the prescribed fraction dose were considered.

Results: For 64 of the 82 patients all local dose differences were smaller than ±5% of the prescribed dose. For 3 patients local dose differences larger than 10% were encountered. The largest dose differences were seen for patients with considerable variations in the amount of gas in their rectum. Other sources of deviations were patient positioning, hip prostheses, and machine output drop at the end of target life. The introduction of GPU based computation for the dose verification software reduced the calculation time from two hours in version 1 to two minutes in version 2. Since November 2011 treatment delivery for prostate patients is only checked by dose reconstruction. Phantom measurements are initiated when large deviations (>6.5% of the prescribed dose) are seen. For 5 out of 27 patients additional phantom measurements were performed, which did not reveal any significant deviations.

Conclusion: Dose reconstruction based on MVCT-detector data yields good agreement with the planned dose distribution. Phantom measurements can be replaced by dose reconstruction, reducing the amount of QA time on the treatment machine. With GPU-based computation, and further development of deformable registration, accurate, on-line dose accumulation may be achievable in the next years.

Author Disclosure: T. Nuver: None. D. Kramer: None. V. Althof: None. R. Westendorp: None. A. Minken: None.

3460

Automatic Adaptive Inverse Planning Optimization for Head-and-Neck Cancer Radiation Therapy

X. Jiang,[1,2] J. Liang,[2] and Y. Di[2]; [1]*Department of Radiation Oncology, West China Hospital, Sichuan University, Chengdu, China,* [2]*Department of Radiation Oncology, William Beaumont Hospital, Royal Oak, MI*

Purpose/Objective(s): Weekly offline adaptive inverse planning optimization needs to be performed during the H&N cancer adaptive radiation therapy. To reduced clinical load, as well as improving planning reliability, we developed an automatic adaptive inverse planning method, and evaluated this method retrospectively by comparing it to the manual adaptive inverse planning.

Materials/Methods: An iterative method was developed for the adaptive inverse planning automation. The expected treatment dose in organs of interest constructed using the previous and on going treatment plans, and daily CBCT images was utilized to setup an initial criteria for each organ in the objective function. Following the initial inverse planning optimization, the achieved objective value was used to modify the previous criteria in the objective with respect to a pre-determined formulation, and then a new inverse planning optimization was repeated accordingly. The iteration was stopped if there was no clear improvement in the objective. The automatic planning method was evaluated using the pre-treatment planning CT and daily CBCT images obtained during the entire treatment course of 10 H&N cancer patients. The evaluation was performed by comparing the total cumulative treatment dose in all organs of interest constructed using the automatic plan and a manual plan respectively. The manual adaptive inverse planning was performed by a single person following a fixed rule on selecting the objective criteria, with the goal to reduce a 5% from the currently achievable normal organ dose-volume parameter obtained from the expected treatment dose.

Results: The adaptive planning was automatically completed for 30% of cases with the average 8 iterations per case. Minor manual adjustment on the target coverage was needed for the other 70% planning. Compared to the treatment dose obtained from the pre-treatment IMRT plan, the mean EUD to cord, brainstem, right parotid, left parotid and mandible with respect to the automatic adaptive plan and the manual adaptive plan decreased 36.0% (0.1%∼48.3%) vs 9.1% (3.6%∼17.2%); 45.4% (31.4∼54.3%) vs 10.2% (2.9%∼19.3%); 23% (8.6%∼33.8%) vs 12.4% (3.1%∼23.2%); 33.5% (24.3%∼50.1%) vs 18.5% (7.6∼23.3%); and 8.9% (2.5%∼12.5%) vs 9.3% (2.0%∼14.1%) respectively.

Conclusion: Our study demonstrated adaptive inverse planning can most likely be performed automatically in clinical implementation. The quality of the automatic planning is commonly superior to the manual planning if "try-n-error" is not thoroughly applied in the manual planning process.

Author Disclosure: X. jiang: None. J. Liang: None. Y. Di: None.

3461

Dose-Mass-based Inverse Optimization for Head-and-Neck Cancers

I.B. Mihaylov,[1] I.B. Mihaylov,[1] and E. Moros[2]; [1]*Rhode Island Hospital, Providence, RI,* [2]*Moffitt Cancer Center, Tampa, FL*

Purpose/Objective(s): It has been argued in the literature that dose-mass-histograms (Dmhs) may be more relevant to radiation therapy than commonly accepted dose-volume-histograms (Dvhs). The widespread use of Dvhs stems from the wealth of clinical information expressed in that form. Furthermore, historically when the Dvhs were introduced the homogenous dose calculations and optimizations were the norm, and thereby no attention was paid to Dmhs. The purpose of this work is to compare Dvh and Dmh inverse optimization results for head-and-neck (HN) cancer.

Materials/Methods: Ten HN patient plans were retrospectively optimized for IMRT. The optimization was performed with Dmh and Dvh based quadratic objective functions. With either optimization nine equally spaced beams were used. Step-and-shoot IMRT with total of 100 segments was used in each plan. The minimum allowed segment area and minimum monitor units (MUs) per segment were set the same for Dmh and Dvh optimization schemes. Both Dmh and Dvh plans were normalized such that 95% of the PTV received the prescription dose. Once prescription was achieved, the doses to organs at risk (OARs) such as spinal cord, brainstem, larynx, left and right parotid glands (OARs) were iteratively lowered until standard deviation of the dose across the PTV in each plan became ∼ 4%. Dose indices (DIs), such as $D^{PTV}_{95\%}$ (dose to 95% of the PTV), $D^{Cord}_{1\%}$, $D^{Brainstem}_{1\%}$, $D^{Larynx}_{50\%}$, $D^{Lt\_parotid}_{50\%}$, and $D^{Rt\_parotid}_{50\%}$ were compared. Percent difference between Dvh- and Dmh-plan derived dose indices were tallied, with the Dmh-derived values used as reference. Therefore, if a DI